Chemical Tracers of Dynamics in Low-Mass Protostellar Objects

Satoshi Yamamoto[1], **Yoko Oya**[1] and **Nami Sakai**[2]

[1]Department of Physics, The University of Tokyo,
Bunkyo-ku, Tokyo, 113-0033, Japan
email: `yamamoto@taurus.phys.s.u-tokyo.ac.jp`, `oya@taurus.phys.s.u-tokyo.ac.jp`

[2]RIKEN, Wako, Saitama, 351-0198, Japan
email: `nami.sakai@riken.jp`

Abstract. Recent progress in astrochemistry of low-mass protostellar sources is reviewed. In particular, we focus on disk formation processes and associated chemical changes at a 50 au scale, which is extensively being studied with ALMA. A small scale chemical differentiation sensitively reflects changes in physical conditions, and hence, it provides us with unique opportunities of chemical diagnostics of disk-forming regions. Complex physical and chemical pictures of disk formation revealed by observations are summarized, and future prospects are discussed.

1. Historical Overview

One of important goals for astrochemistry and astrophysics is to understand chemical evolution from interstellar molecular clouds to planetary systems, which is directly related to the origin of the Solar System. So far, chemical compositions of molecular clouds and star-forming regions have extensively been studied, and their basic properties are reasonably understood. Likewise, chemical compositions of protoplanetary disks have also been explored, although the number of molecular species detected so far is not as many as that for molecular clouds. On the other hand, a link between these two stages, that is chemistry of disk-forming regions, has sparsely been investigated, because of its small size scale as well as physical and chemical complexities. However, ALMA is now changing this situation. Before moving on to the ALMA results on disk-forming regions, progress of astrochemistry of low-mass (solar-type) star-forming regions for the last three decades is overviewed with a particular focus on complex organic species.

1.1. *Early Days*

After discovery of various interstellar molecules in 1970s, chemical difference among observing objects was immediately recognized. Such information was used to choose an appropriate astronomical source for hunting new interstellar molecules. At the same time, chemistry was found to be sensitive to the physical condition of sources, and this characteristic suggested a possibility of chemical diagnostics of star formation to us.

In 1980s, chemistry of star-forming regions was almost equivalent to chemistry of high-mass star-forming regions. Spectral line observations in the millimeter-wave region were extensively conducted toward a few high-mass star-forming regions revealing bright molecular line emission (e.g., Cummins *et al.*1986; Blake *et al.* 1987; Masson & Mundy 1988; Turner 1989). Various large complex organic molecules (COMs) such as $HCOOCH_3$, $(CH_3)_2O$, and C_2H_5CN as well as sulfur-bearing species (SO and SO_2) were detected in a hot ($T > 100$ K) and dense region ($n(H_2) > 10^6$ cm^{-3}) around high-mass young stellar objects, which is called as *hot core* (Herbst & van Dishoeck 2009; Caselli and Ceccarelli

2012 for review). Since the large COMs were only found in hot cores, they were thought to be characteristic species of hot core chemistry.

In contrast, chemistry of low-mass star-forming regions was less studied in those days. Myers and his collaborators systematically studied physical properties of dense cores in dark clouds, and established them as birthplaces of low-mass stars with the aid of the infrared observations with the *IRAS* satellite (e.g. Myers & Benson 1983; Beichman *et al.* 1986; Benson & Myers 1989). However, their chemistry did not attract much attention of astrochemists, because the molecular emission is generally much fainter than that in high-mass star-forming regions. Low-mass version of hot cores was naturally expected, but the spectral lines of large COMs were not detected because of insufficient telescope sensitivity. Suzuki *et al.* (1992) revealed the systematic chemical difference between starless cores and star-forming cores: carbon-chain molecules are abundant in the former, while NH_3 are abundant in the latter. However, this is not the effect of star-formation activities, but mostly due to a combination of a chemical evolutionary effect and depletion of molecules onto dust grains (Suzuki *et al.* 1992; Aikawa *et al.* 2001).

1.2. *Chemistry of Low-Mass Star-Forming Regions*

In 1990s, pioneering works on chemistry of low-mass star-forming regions were reported by Blake *et al.* (1994) and van Dishoeck *et al.*(1995). They conducted a spectral line survey in the 230 and 345 GHz bands toward the low-mass star-forming region IRAS 16293–2422 in Ophiuchus with the CSO 10.4 m telescope and the JCMT 15 m telescope. In this observation, bright lines of sulfur-bearing molecules such as OCS, H_2CS, SO, and SO_2 were detected. In addition, high excitation lines of H_2CO and CH_3OH were also found. Excitation analyses of the observed lines strongly suggest the existence of a hot and dense region (hot core) near the protostar. A hot and dense region around the low-mass protostar was also suggested by the multi-line analysis of H_2CO and CH_3OH toward other protostars (Ceccarelli *et al.* 1998; 2000; Shoier *et al.* 2002). However, the large COMs, $HCOOCH_3$, $(CH_3)_2O$, and C_2H_5CN, which are characteristic to hot cores, were not detected. It should be noted that the distributions of the bright OCS and H_2CS emission in IRAS 16293-2422 were unclear in those days. Their distributions concentrated around the protostar have recently been revealed by Oya *et al.* (2016).

In 2003, Cazaux *et al.* detected the spectral lines of $HCOOCH_3$, $(CH_3)_2O$, and C_2H_5CN toward IRAS 16293–2422 with the IRAM 30 m telescope. This discovery was immediately followed up by interferometric observations, and the distribution of these molecules are found to be concentrated within a few 100 au region around each binary component (Source A and Source B) (Bottinelli *et al.* 2004a; Kuan *et al.* 2004). Thus, a hot-core like chemistry was found to be indeed occurring there. This discovery attracted many researchers in relation to organic materials in meteorites and comets.

It was thought that the above molecules are formed on dust grains and are sublimated in the hot region around the protostar (e.g., Garrod and Herbst, 2006; Aikawa *et al.* 2008; Herbst & van Dishoeck 2009). Later, it was also pointed out that they could be formed by gas-phase reactions starting from CH_3OH and H_2CO sublimated from dust grains (e.g. Balucani *et al.* 2015). The size of the hot region around a low-mass protostar is so tiny in comparison with a hot core around a high-mass protostar that it is named as *'hot corino'* (Bottinelli *et al.* 2004b). Extensive searches of hot corinos were conducted with large single dish telescopes, but only a few definitive hot corinos harboring the large COMs were found after IRAS 16293–2422. Those are NGC1333 IRAS 2A (Jørgensen *et al.* 2005), NGC1333 IRAS4A (Bottinelli *et al.* 2004b), NGC1333 IRAS4B (Sakai *et al.* 2006; Bottinelli *et al.* 2007), Serpens SMM1, and Serpens SMM4 (Öberg *et al.* 2011).

1.3. *Discovery of Chemical Diversity in Low-Mass Protostellar Sources*

In the course of a sensitive search for hot corinos, Sakai *et al.* (2008) discovered a protostellar source, whose chemical composition is completely different from the hot corino sources. It is L1527 in Taurus. In this source, carbon-chain molecules and their related species are extremely rich in a few 1000 au region around the protostar (Sakai *et al.* 2010). In general, carbon-chain molecules are only abundant in young starless cores, while they are deficient in protostellar cores (e.g., Suzuki *et al.* 1992; Aikawa *et al.* 2001). Hence, association of carbon-chain molecules around the protostar was very surprising. Sakai *et al.* (2008) proposed that carbon-chain molecules are *in situ* produced in the gas phase of a warm (> 25 K) region around the protostar by sublimation of CH_4 from grain mantle. This mechanism is named as *warm carbon-chain chemistry* (WCCC). An essential part of it was indeed confirmed by the chemical models (Hassel *et al.* 2008; Aikawa *et al.* 2008). Soon after the discovery of L1527 as the WCCC source, another protostar in Lupus, IRAS 15398–3359 was identified as the second WCCC source (Sakai *et al.* 2009).

In contrast to the rich existence of carbon-chain molecules, the large COMs are not detected in the WCCC sources, although L1527 harbors the Class 0-I protostar as in the case of the hot corino sources. This fact means that chemical compositions of protostellar cores have significant diversity even among the sources in similar evolutionary stages. The diversity can readily be seen as the different spectral appearance between IRAS 16293–2422 and L1527 (Figure 1). Since both hot corino chemistry and WCCC are triggered by evaporation of grain mantle, chemical compositions of grain mantle have to be different between these two cases. Sakai *et al.* (2009) proposed that a different duration time of the starless-core phase after shielding the interstellar UV radiation will make such a difference of grain mantle compositions. A shorter duration time favors WCCC, while a longer duration time results in hot corino chemistry. This situation is schematically shown in Figure 2. If this is the case, the chemical composition of protoatellar cores tells about the history of their starless-core phase which was memorized in the chemical composition of grain mantle. This would be a novel contribution of chemistry to star formation studies.

However, only a few definitive hot corino sources and a few definitive WCCC sources were recognized by single dish observations. This is partly due to insufficient sensitivity of the telescopes employed. In addition, the existence of intermediate character sources is suggested by survey observations of protostellar sources (Sakai *et al.* 2009; Sakai & Yamamoto 2013). Hence, it is still controversial what is the standard chemical composition for protostellar cores. It is also interesting how the chemical diversity in the protostellar cores is handed over to protoplanetary disks and eventually to planets. In 2011, ALMA started its early science operation, and is addressing these issues.

2. New Results with ALMA

2.1. *Detection of More Hot Corinos*

Thanks to high sensitivity and high angular resolution capabilities of ALMA, new hot corino sources have been detected. Codella *et al.* (2016) detected the CH_3CHO lines toward the low-mass protostellar source HH212 at a subarcsecond resolution with ALMA. This is a Class 0 protostar in Orion ($d = 400$ pc), showing a well collimated outflow (Codella *et al.* 2014; Lee *et al.* 2014; Podio *et al.* 2015; Lee *et al.* 2017). The distribution of CH_3CHO is concentrated around the protostar, and is similar to that of HDO. The line shape of CH_3CHO is also similar to that of HDO, whose line width is as broad as 7 km s^{-1}. Since HDO is thought to sublimated from grain mantle, the similarities between
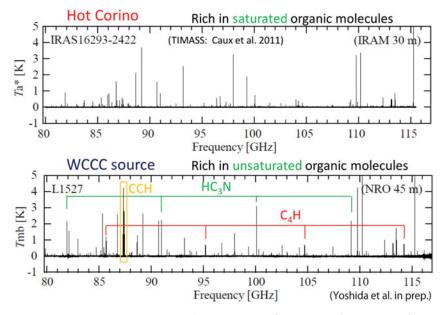
Figure 1. Spectral line surveys toward IRAS 16293–2422 (upper panel) and L1527 (lower panel). The spectrum patterns for the two sources are significantly different. Note that the lines appear to be weaker by a factor of about 2 due to insufficient spectral resolution of the spectrometer in the L1527 survey.
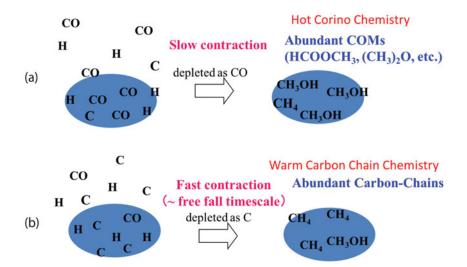

Figure 2. A proposed scenario to account for the chemical variation which we observe in low-mass star-forming cores (Sakai *et al.* 2009; Sakai & Yamamoto 2013). Sketch (a) represents the long starless-core phase which favors hot corino chemistry. In this case, most of the C atoms are converted to the CO molecules in the gas phase, which then deplete onto dust grains. They then form CH_3OH, H_2CO, and more complex organic molecules through hydrogenation reactions and radical reactions on the grain surfaces. Large COMs such as $HCOOCH_3$ may also be produced from CH_3OH and H_2CO in the gas phase after their evaporation. Sketch (b) represents a short starless-core phase in which most of the C atoms deplete directly onto the dust grains, and then form CH_4 through hydrogenation. This favors WCCC, with carbon-chain molecules produced in the gas phase after evaporation of CH_4 from dust grains.

CH_3CHO and HDO mean that CH_3CHO also exists in the hot and dense region near the porotstar. This is the first discovery of a hot corino in Orion. Recently, Lee *et al.* (2017) reported the detection of NH_2CHO in this source with ALMA.

Imai *et al.* (2016) also detected CH_3CHO, $HCOOCH_3$ and NH_2CHO toward the isolated low-mass protostar IRAS 19347+0727 in the Bok globule B335 ($d = 100$ pc) with ALMA. This source is well known as an ideal test-bed for star formation studies, and physical structures of its parent dense core and the associated outflow have extensively been studied (e.g., Hirano *et al.* 1988; Chandler and Sargent 1993; Evans *et al.* 2015; Yen *et al.* 2015). In contrast, studies on its chemical composition are relatively sparse, although the chemical composition at a few 1000 au scale was explored by observing fundamental molecules (Evans *et al.* 2005). The distribution of COMs is found to be concentrated around the protostar, which is unresolved with the $0\rlap{.}''5$ (50 au) beam of ALMA. The outflow of this source is extending almost along the plane of sky, and hence, the envelope/disk structure likely has the edge-on configuration. Nevertheless, a rotation signature is not recognized. Thus, the broad spectral line profile of COMs suggests that the COM emission most likely comes from the infalling gas in the vicinity of the protostar. The fractional abundances relative to H_2 are derived to be 2.4×10^{-9}, 4.3×10^{-10}, and 4.6×10^{-9} for CH_3CHO, NH_2CHO, and $HCOOCH_3$, respectively. They are almost comparable to those found in the other hot corions (e.g., Taquet *et al.* 2015), and hence, B335 can be recognized as a hot corino source.

2.2. *Physical and Chemical Structures of Protostellar Cores: L1527*

Sakai *et al.* (2014a) observed the prototypical WCCC source L1527 with ALMA. This source has an almost edge-on disk/envelope system extending along the north-to-south direction and the extended outflow blowing the east and west directions (Ohashi *et al.* 1997; Hogerheijde *et al.* 1998; Tobin *et al.* 2013). Although carbon-chain molecules were known to be concentrated around the protostar at a 1000 au scale, its detailed distribution and kinematic structure at a smaller scale was unclear. The ALMA observation revealed that the distribution of the carbon-chain related species c-C_3H_2 is elongated along the inner part of the flattened envelope (Figure 3a). The kinematic structure clearly indicates the rotating motion of the envelope, as shown in the position-velocity diagram of Figure 3b. The rotation profile abruptly disappears inside the radius of 100 au from the protostar. In addition, the infalling gas is apparently visible toward the protostar. Hence, the kinematic structure traced by the c-C_3H_2 line cannot be explained by the Keplerian motion, but by an infalling-rotating gas conserving the angular momentum.

Figure 3c shows the simulation result for the infalling-rotating envelope model assuming the ballistic motion (Oya *et al.* 2014; 2015). The model result well reproduces the observed positon-velocity diagrams. The radius inside which the rotation profile disappears is thus found to be the radius of the centrifugal barrier of the infalling-rotating envelope. When the gas motion is approximated by the ballistic motion, the gas cannot fall inward of a certain radius because of the conservation of energy and angular momentum. This perihelion radius is called as the centrifugal barrier. It corresponds to a half of the centrifugal radius, where the centrifugal force balances to the gravity of the central star. The outgoing gas from the centrifugal barrier collides with the infalling gas, and hence, a week accretion shock will occur in front of the centrifugal barrier. As a result, the gas is stagnated there. If the angular momentum of the gas around the centrifugal barrier is extracted by some mechanisms such as disk winds and slow molecular outflows, a part of the gas can further fall toward the protostar to form a rotationally supported (Keplerian) disk inside the centrifugal barrier. The distribution of c-C_3H_2 clearly shows that this molecule is present in the infalling-rotating envelope, and is absent in the disk

component. Sakai *et al.* (2014b) also revealed that CCH and CS shows the similar distribution. Carbon-chain related molecules and CS are thought to be frozen out onto dust grain in the mid-plane of the disk component, where the density is as high as 10^8 cm^{-3} and the temperature is as low as 30 K.

Figure 3d shows the position-velocity diagram of the SO line observed with ALMA (Sakai *et al.* 2014a). In contrast to c-C$_3$H$_2$, the distribution of SO is concentrated around the centrifugal barrier, as revealed by the bar-shaped feature in the position-velocity diagram. SO does not exist in the infalling-rotating envelope. Thus, a drastic chemical change is occurring around the centrifugal barrier. SO seems to be liberated from grain mantle by the weak accretion shock expected around the centrifugal barrier. It should be noted that a component having higher velocity than the maximum velocity at the centrifugal barrier can marginally be seen inside the centrifugal barrier. This may indicate the existence of SO in the disk component. Although both CS and SO are sulfur-bearing molecules, their distributions are found to be much different at a disk-formation scale in L1527. Note that a similar SO distribution was also reported by Ohashi *et al.* (2014).

On the other hand, the distribution of H$_2$CO is different from those of the above molecules (Sakai *et al.* 2014b). The position velocity diagram of H$_2$CO clearly shows the high velocity component associated with the disk component inside the centrifugal barrier in addition to the infalling-rotating envelope component and its centrifugal barrier.

The above results for L1527 shows the chemical differentiation around the low-mass protostars at a 50 au scale. More importantly, the chemical differentiation is related to the physical transition from the infalling-rotating envelope to the disk component. In other words, the disk formation around low-mass protostars can be studied by chemical diagnostics. For such studies, L1527 can be regarded as a *Rosetta Stone*, which allows us to translate the chemical compositions to the physical structures.

2.3. *The Other WCCC Sources*

Indeed, a similar chemical differentiation was found in the evolved WCCC source IRAS 04365+2535 in TMC-1A ($d = 140$ pc) (Sakai *et al.* 2016). This is a Class I protostar harboring rich carbon-chain molecules. The CS emission clearly traces the infalling-rotating envelope, while the SO emission selectively traces the centrifugal barrier. Although the distributions of CS and SO are asymmetric around the protostar, the essential feature of the chemical differentiation is similar to the L1527 case. With the aid of the ballistic model, the radius of the centrifugal barrier is determined to be 50 au. The gas certainly keeps falling beyond the centrifugal radius (100 au) in this source. The result contrasts the disk radius of 100 au inferred from the analysis of the C^{18}O data (Aso *et al.* 2016). This contradiction would come from the complex physical structure in the transition zone (Section 3), which is ignored in their analysis.

Another WCCC source IRAS 15398–3359 shows a similar trend (Oya *et al.* 2014). In this source, the CCH and H$_2$CO distributions were studied. The both molecules trace the disk/envelope component as well as the outflow cavity. The integrated intensity distribution of the CCH emission shows a marginal dip toward the porotostar, while that of H$_2$CO has a clear peak at the protostar. This trend is consistent with that found in L1527, although the velocity gradient was not detected clearly at a resolution of 0″.5, because of the small protostar mass and the small radius of the centrifugal barrier.

The rotating ring traced by the SO emission is also found for L1489 by Yen *et al.* (2014). This source is a Class I protostar in Taurus, and the Keplerian disk structure is reported. The position velocity diagram of SO shows a bar-like feature, indicating the rotating ring with the radius of 300 au. Unfortunately, no carbon-chain molecules and CS were observed for this source, and the infalling-rotating envelope was not characterized.
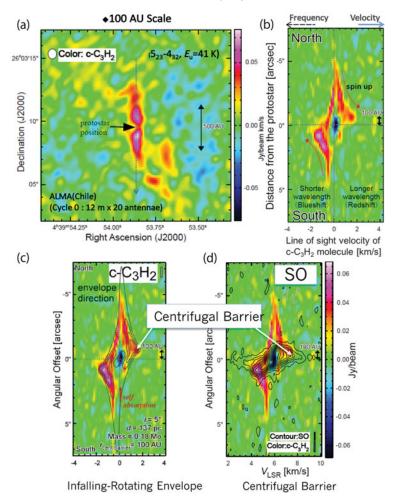
Figure 3. (a) Integrated intensity distribution of the c-C$_3$H$_2$ ($5_{2,3} - 4_{3,2}$; 249 GHz) line. (b) Position-velocity diagram of the c-C$_3$H$_2$ line along the north-to-south direction shown in panel (a) by the dashed arrow. (c) Position-velocity diagram of the infalling-rotating envelope model (contours) superposed on that of the c-C$_3$H$_2$ line (color). Contours are every 20% of the peak intensity. (d) Position-velocity diagram of the SO ($J_N = 7_8 - 6_7$; 341 GHz; contours) line superposed on that of the c-C$_3$H$_2$ line (color). Contours are every 4σ (28 mJy beam^{-1}), starting from 2σ. Taken from Sakai *et al.* (2014a; b).

Nevertheless, the SO ring may trace the centrifugal barrier, as in the case of L1527 and TMC-1A.

2.4. *Hot Corino Sources*

We now know the small scale chemical differentiation for the WCCC sources. Then what about hot corino sources? To address this question, Oya *et al.* (2016) studied the physical and chemical structures of IRAS 16293–2422 Source A in detail with ALMA. As mentioned in Section 1.2, IRAS 16293–2422 is a prototypical hot corino source, toward which various molecular-line observations have been carried out (e.g., Cazaux *et al.* 2003; Caux *et al.* 2011; Jørgensen *et al.* 2016). As presented in this symposium (Oya 2017), the kinematic structure of this source is well represented by an infalling rotating envelope and a Keplerian disk component inside it. The OCS line selectively traces the

infalling-rotating envelope, while the CH_3OH and $HCOOCH_3$ lines highlight the centrifugal barrier. On the other hand, H_2CS exists in the infalling-rotating envelope and the disk component. Although the chemical species tracing each part is different from those for the WCCC sources, the chemical differentiation at a 50 au scale is evident in IRAS 16293–2422 Source A. An essentially similar chemical structure is also found for the companion Source B (Oya *et al.* 2018). CH_3OH and large COMs seem to be evaporated from grain mantle around the centrifugal barrier due to accretion shock of the infalling gas and/or direct heating by protostellar radiation. A faint high velocity component seen in these molecules implies that they would survive even in the disk component to some extent. Thus, a drastic chemical change is also occurring around the centrifugal barrier in the hot corino sources, as in the WCCC sources.

Very recently, Lee *et al.* (2017) revealed the distributions of HCO^+, CH_3OH, CH_2DOH, CH_3SH, and NH_2CHO in the hot corino source HH212 with ALMA. At a very high angular resolution of $0\rlap{.}{''}04$, the distributions of these molecules including those of the vertical direction to the disk/envelope structure were beautifully resolved. The HCO^+ emission is found to trace the infalling-rotating envelope down to its centrifugal barrier, while CH_3OH and other organic species the atmosphere of the disk within the centrifugal barrier. This result is almost consistent with those found in IRAS 16293–2422 (Oya *et al.* 2016), and further reminds us the complex physical and chemical nature in the disk-forming region.

2.5. *Discovery of Hybrid Chemical Character Sources*

According to the proposed scenario of the chemical diversity (Figure 2), intermediate or hybrid character sources should naturally be expected. Although their presence is suggested by the survey observations with single-dish telescopes (Sakai *et al.* 2009), they were not identified at a high angular resolution. Oya *et al.* (2017) identified L483 as an example of such sources for the first time. L483 harbors the Class 0 protostar, IRAS 18148-0440, whose bolometric luminosity is as high as 13 $L_\odot$. It is located in Aquila Rift at the distance of 200 pc. This source was considered to be a WCCC candidate source, because carbon-chain molecules such as C_4H_2 and l-C_3H_2, which are usually undetected in protostellar cores, were detected (Hirota *et al.* 2009; Sakai *et al.* 2009). With ALMA, Oya *et al.* (2017) indeed confirmed the association of CCH extended over a few 100 au scale around the protostar, confirming the WCCC nature of this source. Its distribution has a hole toward the protostar position. Since the signal-to-noise ratio of the CCH emission is not enough to study its kinematic structure, we instead studied the kinematic structure of the CS line. Figure 4a shows the position velocity diagram of CS along the envelope/disk direction, while Figures 4b and c represent the simulation results of the infalling-rotating envelope and Keplerian models, respectively. Although CS traces the infalling-rotating envelope, it also traces the disk component inside the centrifugal barrier. In addition, SO traces the disk component inside the centrifugal barrier (Figure 4d). These features are in contrast to the L1527 and TMC-1A cases. This may be due to the high luminosity of this source, which prevents CS and SO from freezing out onto dust grains in the mid-plane of the disk component. Moreover, they detected the spatially-unresolved emission of $HCOOCH_3$, HNCO, and NH_2CHO toward the protostar. The detection of COMs clearly indicates the hot corino activity in this source. Hence, L483 can be regarded as the first source which definitively possesses both the WCCC and hot corino characters. Since WCCC is triggered by evaporation of CH_4, it is caused in the extended warm part ($T > 25$ K) of the protostellar core. On the other hand, evaporation of COMs, which characterizes the hot corino activity, only occurs in a hot part ($T > 100$
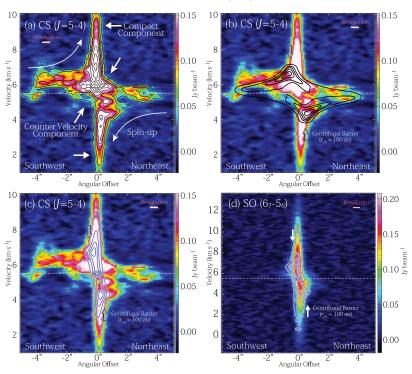
Figure 4. (a) Position-velocity diagram of the CS ($J = 5 - 4$) line along the envelope/disk direction. Contours are every 5σ (38 mJy beam^{-1}). (b) Position-velocity diagram of the in-falling-rotating envelope model (contours) superposed on that of the CS line (color). Contours are every 20% from 5% of each peak intensity. (c) Position-velocity diagram of the Keplerian model (contours) superposed on that of the CS line (color). Contours are every 20% from 5% of each peak intensity. (d) Position-velocity diagram of the SO ($J_N = 6_7 - 5_6$; color) line and the Keplerian model (contours). Contours are every 30% from 3% of the peak intensity.

K) near the protostar. Such a difference of the distributions of CCH and COMs is indeed seen in L483.

A similar hybrid character has recently been recognized for B335. As mentioned above, this source harbors an unresolved hot corino. It also shows the relatively bright CCH emission concentrated at a 1000 au scale around the protostar. Since the CCH emission is almost absent or very faint in the vicinity of the other hot corino sources (IRAS 16293–2422 Source A, NGC 1333 IRAS 4A), B335 seems to have the WCCC character in addition to the hot corino character, as in the case of L483.

Such a hybrid character is predicted by the chemical model calculation by Aikawa *et al.* (2008). This model adopts the realistic physical model of a star-forming cloud, and simulates the temporal variation of the chemical structure. Their model indeed shows the enhancement of carbon-chain related species in the gas phase around the evapora-tion region of CH$_4$ ($T > 25$ K). This shows the WCCC character. On the other hand, CH$_3$OH and COMs are evaporated in the inner region at higher temperature ($T > 100$ K). Although the model does not consider the complex transition zone from the infalling-rotating envelope to the disk component, the result qualitatively explains the observa-tional results for L483 and B335. The hybrid character source may be a more common occurrence in chemical compositions of protostellar cores. Further ALMA observations to characterize chemical properties of various protostellar cores are thus important.

3. What we have found and what we do not understand?

The infalling-rotating envelope and its centrifugal barrier are clearly demonstrated by molecular line observations. This fact means that the dynamic pressure of the infalling gas is higher than the static pressure and the magnetic pressure in infalling-rotating envelopes at least for L1527, TMC-1A, IRAS 16293–2422 Source A and B, and L483. For this reason, the gas keeps infalling through the centrifugal radius down to the radius of the centrifugal barrier. Then the gas is stagnated in front of the centrifugal barrier, and the accreting gas causes a weak shock there. The broadening of the envelope thickness around the centrifugal barrier is indeed found by the recent high resolution observation (Sakai *et al.* 2017). Inside the centrifugal barrier, the disk structure is expected to grow up. For the disk growth, the angular momentum of the accreting gas has to be extracted by some mechanisms such as disk wind or slow molecular outflows (e.g. Alves *et al.* 2017; Zhao *et al.* 2016; Codella *et al.* 2014). Thus, the transition from the infalling-rotating envelope and the disk component is occurring between the centrifugal radius to the centrifugal barrier, and seems to cause a complex physical structure and kinematics. Observations of the popular gas tracers such as the CO isotopologue lines at a limited angular resolution often tend to smear out the critical structural changes in the transition zone, because such tracers observe everything. On the other hand, chemical changes associated with the transition zone clearly highlight individual parts in the transition zone, just as chemical markers. Since the detailed understandings of the transition zone including its vertical structures are the central issue for the disk formation studies, such chemical approaches will be more and more important.

It should be noted, however, the infalling-rotating envelope model may not always be valid. In a very low mass protostar or a very young protostar, for instance, the central mass is so small that the dynamic pressure caused by the central gravity may not dominate the static pressure and the magnetic pressure. We need further considerations for these cases. In addition, the centrifugal barrier may appear at a much larger radius than a 50 au scale, if the angular momentum of the infalling gas is larger.

The transition zone is not only for physics but also for chemistry. Chemical compositions of the gas drastically change in the transition zone. So far, it has been thought that gas and dust in molecular clouds are smoothly delivered to protoplanetary disks. In fact, the chemical composition of molecular clouds is assumed as the initial condition for the chemical model simulation of protoplanetary disks (e.g., Walsh *et al.* 2014). However, the discovery of the centrifugal barrier and the associated chemical change clearly indicates that such a smooth transition picture is too simplified. In other words, the chemical composition at the centrifugal barrier both in the gas phase and on the surface provide us with the observational constraint to the initial condition of the model. Thus, we need to consider the chemical processes in the transition zone more seriously.

However, it is not well understood what chemical processes are actually occurring in the transition zone. Looking at the tracer molecules for the hot corino and WCCC sources, we recognize that the sulfur-bearing molecules reveals characteristic features. For instance, CS and SO behaves exclusively in the WCCC sources. The fact that OCS traces the infalling-rotating envelope in hot corino sources has not been expected in chemical models. Importance of the sulfur chemistry is often pointed out in various situations (e.g. Wakelam *et al.* 2011). It is also recognized in the analysis of the *Rosetta* data of 67P/Churyumov-Grasimenco (Calmonte *et al.* 2016). However, formation pathways of sulfur bearing species are quite uncertain both in the gas phase and on the grain surface. Thus, a thorough understanding of the sulfur chemistry is urgent.

Another remaining issue is how the isotope fractionation found in cold molecular clouds is transferred to the disk component. The isotope anomaly of molecules is widely recognized in cold interstellar medium, and is expected to be an important tracer which bridges interstellar chemistry and planetary chemistry. In particular, deuterium fractionation of water is extensively studied (e.g., Coutens *et al.* 2012). As for the other molecules, Murillo *et al.* (2015) studied the distribution of DCO^+ in the low-mass protostellar source VLA 1623. According to their result, DCO^+ is distributed in the outer envelope at a few 100 au scale, which shows a rotation signature. On the other hand, it is almost absent in the vicinity of the protostar. Yoshida *et al.* (2017) studied the D_2CO/H_2CO ratio in L1527. The D_2CO distribution peak is found to be offset from the protostar position, while the H_2CO is centrally peaked. Hence, the deuterium fractionation ratio seems to be lower in the disk-forming region. In contrast, Lee *et al.* (2017) very recently reported the detection of CH_2DOH in HH212, as mentioned above. The CH_2DOH distribution is almost the same as the CH_3OH distribution, and hence, substantial deuterium fractionation is seen even around the centrifugal barrier in this source. Hence, it is still controversial how deuterium fractionation changes in the disk formation process. Further observations with ALMA will answer this question.

4. Concluding Remarks

The ALMA observations briefly overviewed above reveal very complex physical and chemical processes occurring in disk-forming regions, most of which have not been anticipated before the ALMA era. More importantly, chemistry is further confirmed to be a powerful diagnostic tool of physical processes around the protostar at a 50 au scale. Such chemical approaches will be a major trend of star-formation studies in the next decade. In addition, we hope that the observational results will give rise to new research activities in molecular physics and chemistry.

5. Acknowledgements

References

Aikawa, Y., Ohashi, N., Inutsuka, S. *et al.* 2001, *ApJ*, 552, 639.
Aikawa Y., Wakelam, V., Garrod, R. T., & Herbst, E. 2008, *ApJ*, 674, 993.
Alves, F. O., Girart, J. M., Caselli, P. *et al.* 2017, *A&A*, 603, L3.
Aso, Y., Ohashi, N., Saigo, K. *et al.* 2015, *ApJ*, 812, 27.
Beichman, C. A., Myers, P. C., & Emerson, J. P. 1986, *ApJ*, 307, 337.
Benson, P. J. & Myers, P. C. 1989, *ApJS*, 71, 89.
Blake, G. A., Sutton, E. C., Masson, C. R., & Phillips, T. G. 1987, *ApJ*, 315, 621.
Blake, G. A., van Dishoeck, E. F., Jansen, D. J., *et al.* 1994, *ApJ*, 428, 680.
Bottinelli, S., Ceccarelli, C., Neri, R. *et al.* 2004a, *ApJ*, 617, L69.
Bottinelli, S., Ceccarelli, C., Lefloch, B. *et al.* 2004b, *ApJ*, 615, 354.
Bottinelli, S., Ceccarelli, C., Williams, J. P., & Lefloch, B., 2007, *A&A*, 463, 601.
Balucani, N., Ceccarelli, C., & Taquet, V. 2015, *MNRAS*, 449, L16.
Calmonte, U., Altwegg, K., Balsiger, H. *et al.* 2016, *MNRAS*, 462, S253.
Caselli, P. & Ceccarelli, C. 2012, *Astron. Ap. Rev.* 20, 56.
Caux, E., Kahane, C., Castets, A., *et al.* 2011, *A&A*, 532, A23.
Cazaux, S., Tielens, A. G. G. M., Ceccarelli, C. *et al.* 2003, *ApJ*, 593, L51.
Ceccarelli, C., Castets, A., Loinard, L. *et al.* 1998, *A&A*, 338, L43.

Ceccarelli, C., Loinard, L., Castets, A. *et al.* 2000, *A&A*, 357, L9.

Chandler, C. J. & Sargent, A. I. 1993, *ApJL*, 414, L29.

Codella, C., Cabrit, S., Gueth, F. *et al.* 2014, *A&A*, 568, L5.

Codella, C., Ceccarelli, C., Cabrit, S. *et al.* 2016, *A&A*, 586, L3.

Coutens, A., Vastel, C., Caux, E. *et al.* 2012, *A&A*, 539, A132.

Cummins, S. E., Linke, R. A., & Thaddeus, P. 1986, *ApJS*, 60, 819.

Evans, N. J., II, Lee, J.-E., Rawlings, J. M. C., & Choi, M. 2005, *ApJ*, 626, 919

Evans, N. J., II, Di Francesco, J., Lee, J., *et al.* 2015, *ApJ*, 814, 22

Garrod, R. T. & Herbst, E. 2006, *A&A*, 457, 927.

Hassel, G. E., Herbst, E., & Garrod, R. T. 2008, *ApJ*, 681, 1385.

Herbst, E. & van Dishoeck, E. F. 2009, *ARAAp*, 47, 427.

Hirano, N., Kameya, O., Nakayama, M., & Takakubo, K. 1988, *ApJL*, 327, L69.

Hirota, T., Ohishi, M., & Yamamoto, S. 2009, *ApJ*, 699, 585.

Hogerheijde, M. R., van Dishoeck, E. F., Blake, G. A. *et al.* 1998, *ApJ*, 502,315.

Imai, M., Sakai, N., Oya, Y. *et al.* 2016, *ApJL*, 830, L37.

Jørgensen, J. K., Bourke, T. L., Myers, P. C. *et al.* 2005, *ApJ*, 632, 973.

Jørgensen, J. K., van del Wiel, M. H. D., Coutens, A. *et al.* 2016, *A&A*, 595, A117.

Kuan, Y.-J., Huang, H.-C., Charnley, S. B. *et al.* 2004, *ApJ*, 616, L27.

Lee, C.-F., Hirano, N., Zhang, Q., *et al.* 2014, *ApJ*, 786, 114.

Lee, C.-F., Li, Z.-Y., Ho, P. T. P.. *et al.* 2017, *ApJ*, 843, 27.

Masson, C. R. & Mundy, L. G. 1988, *ApJ*, 324, 538.

Murillo, N. M., Bruderer, S., van Dishoeck, E. F. *et al.* 2014, *A&A*, 579, A114.

Myers, P. C. and Benson, P. J. 2003, *ApJ*, 266, 309.

Öberg, K., van der Marel, N., Kristensen, L. E., & van Dishoeck, E. F. 2011, *ApJ*, 740, 14.

Ohashi, N., Hayashi, M., Ho, P. T. P., & Momose, M. 1997, *ApJ*, 475, 211.

Ohashi, N., Saigo, K., Aso, Y., *et al.* 2014, *ApJ*, 796, 131.

Oya, Y., Sakai, N., Sakai, T. *et al.* 2014, *ApJ*, 795, 152.

Oya, Y., Sakai, N., Lefloch, B. *et al.* 2015, *ApJ*, 812, 59.

Oya, Y., Sakai, N., López-Sepulcre, A. *et al.* 2016, *ApJ*, 824, 88.

Oya, Y. 2017, *Proceedings of IAU Symposium* No. 332.

Oya, Y., Moriwaki, K., Onishi, S. *et al.* 2018, *ApJ*, 854, 96.

Oya, Y., Sakai, N., Watanabe, Y. *et al.* 2017, *ApJ*, 837, 174.

Podio, L., Codella, C., Gueth, F., *et al.* 2015, *A&A*, 581, 85.

Sakai, N., Sakai, T., & Yamamoto, S. 2006, *PASJ*, 58, L15.

Sakai, N., Sakai, T., Hitora, T., & Yamamoto, S. 2008, *ApJ*, 672, 371.

Sakai, N., Sakai, T., Hirota, T. *et al.* 2009, *ApJ*, 697, 769.

Sakai, N., Sakai, T., Hirota, T., & Yamamoto, S. 2010, *ApJ*, 722, 1633.

Sakai, N. & Yamamoto, S. 2013, *ChRv*, 113, 8981.

Sakai, N., Sakai, T., Hirota, T., *et al.* 2014a, *Natur*, 507, 78.

Sakai, N., Oya, Y., Sakai, T., *et al.* 2014b, *ApJL*, 791, L38.

Sakai, N., Oya, Y., López-Sepulcre, A., *et al.* 2016, *ApJL*, 820, L34.

Sakai, N., Oya, Y., Higuchi, A. E. *et al.* 2017, *MNRAS*, 467, L76.

Schoier, F. L., Jørgensen, J. K., van Dishoeck, E. F., & Blake, G. A. 2002, *A&A*, 390, 1001.

Suzuki, H., Yamamoto, S., Ohishi, M. *et al.* 1992, *ApJ*, 392, 551.

Taquet, V., López-Sepulcre, A., Ceccarelli, C., *et al.* 2015, *ApJ*, 804, 81.

Tobin, J. J., Hartman, L., Chiang, H.-F. *et al.* 2013, *ApJ*, 771, 48.

Turner, B. E. 1989, *ApJS*, 70, 539.

van Dishoeck, E. F., Blake, G. A., Jansen, D. J., & Groesbeck, T. D. 1995, *ApJ*, 447, 760.

Wakelam, V., Hersant, F., & Herpin, F. 2011, *A&A*, 529, A112.

Walsh, C., Millar, T. J., Nomura, H. *et al.* 2014, *A&A*, 563, A33.

Yen, H. W., Takakuwa, S., Ohashi, N., *et al.* 2014, *ApJ*, 793, 1.

Yen, H. W., Takakuwa, S., Koch, P. M., *et al.* 2015, *ApJ*, 812, 129.

Yoshida, K., Sakai, N., Yamamoto, S. *et al.* 2017, in preparation.

Zhao, B., Caselli, P., Li, Z.-Y. *et al.* 2016, *MNRAS*, 460, 2050.